

$^{14}\text{NO}_3^-$  data for this period indicates that endogenous synthesis contributes 7  $\mu\text{mole}$  of urinary  $\text{NO}_3^-$ . Since this is less than the 9  $\mu\text{mole}$  of dietary  $\text{NO}_3^-$  that do not appear in the urine, the net excretion of  $\text{NO}_3^-$  is now less than the amount ingested. Thus, although  $\text{NO}_3^-$  synthesis occurs at all concentrations of  $\text{NO}_3^-$  intake, urinary excretion in excess of intake will be apparent only when intake is low—that is, when the amount of dietary  $\text{NO}_3^-$  not appearing in the urine is less than the amount of endogenously synthesized  $\text{NO}_3^-$  that is excreted.

Synthesis of  $\text{NO}_3^-$  in humans has been reported (4) and was attributed to intestinal nitrifying bacteria. Our studies indicate that  $\text{NO}_3^-$  synthesis occurs in the germfree rat as well as in the conventional rat and thus is independent of the flora. It appears that  $\text{NO}_3^-$  synthesis is a mammalian process.

LAURA C. GREEN

STEVEN R. TANNENBAUM

Department of Nutrition and Food Science, Massachusetts Institute of Technology, Cambridge 02139

PETER GOLDMAN

Department of Pharmacology, Harvard Medical School, and Beth Israel Hospital, Boston, Massachusetts 02215

#### References and Notes

1. Before it can serve as a nitrosating agent,  $\text{NO}_2^-$  must be reduced to  $\text{NO}_2$ . This reduction is mediated by the microflora of both the oral cavity [B. Spiegelhalder, G. Eisenbrand, R. Preussmann, *Food Cosmet. Toxicol.* **14**, 545 (1976); S. R. Tannenbaum, M. Weisman, D. Fett, *ibid.* **14**, 549 (1976)] and the achlorhydric stomach [W. S. J. Ruddell, E. S. Bone, M. J. Hill, C. L. Walters, *Lancet* **1**-1978, 521 (1978)]. Nitrite is not normally found in blood or urine, however, because it is rapidly oxidized to  $\text{NO}_3^-$  by oxyhemoglobin [H. Kosaka, K. Imaizumi, K. Imai, I. Tyuma, *Biochim. Biophys. Acta* **581**, 184 (1979)].
2. See the review by P. N. Magee, R. Montesano, and R. Preussmann [Chemical Carcinogens (Monograph 172, American Chemical Society, Washington, D.C. 1976), p. 491].
3. H. H. Mitchell, H. A. Shonle, H. S. Grindley, *J. Biol. Chem.* **24**, 461 (1916); M. Kurzer and D. H. Calloway, *Fed. Proc. Fed. Am. Soc. Exp. Biol.* **38**, 607 (1979); J. L. Radomski, C. Palmiri, W. L. Hearn, *Toxicol. Appl. Pharmacol.* **45**, 63 (1978); B. Bartholomew, C. Caygill, R. Darbar, M. J. Hill, *Proc. Nutr. Soc.* **38**, 124A (1979).
4. S. R. Tannenbaum, D. Fett, V. R. Young, P. D. Land, W. R. Bruce, *Science* **200**, 1487 (1978).
5. Biomix 1435 (Bio Serv, Inc., Frenchtown, N.J.). The diet meal was autoclaved for 25 to 35 minutes and stored either refrigerated for the conventional animals or inside the isolator for the germfree animals. Each batch of diet contained no detectable  $\text{NO}_2^-$  (lower detection limit, 50 ng of  $\text{NaNO}_2$  per gram of diet) and at most 2.0  $\mu\text{g}$  of  $\text{NaNO}_3$  per gram of diet.
6. L. A. Wheeler, F. B. Soderberg, P. Goldman, *J. Pharmacol. Exp. Ther.* **194**, 135 (1975).
7. E. Combe, in *Germfree Research: Biological Effects of Gnotobiotic Environments*, J. Hengeman, Ed. (Academic Press, New York, 1973), p. 305.
8. L. C. Green, J. Glogowski, P. Skipper, S. R. Tannenbaum, in preparation.
9. J. W. Tesch, W. R. Rehg, R. E. Sievers, *J. Chromatogr.* **126**, 743 (1976).
10. We used the 5992 GC-MS system (Hewlett-Packard, Palo Alto, Calif.). The GC conditions were as follows: stainless steel column, 1.8 m by 0.32 cm, packed with 6 percent OV 225 Porapak

- Q, 100/120 mesh; carrier flow, 25 ml of helium per minute; temperature, 170°C; retention time, 1.5 minutes. The MS conditions consisted of selected ion monitoring at a mass-to-charge ratio (*m/e*) of 123 ( $\text{M}^+$ ) and *m/e* 124 ( $\text{M} + 1^+$ ). Complete spectra of samples and nitrobenzene standards were also run to confirm the identity.
11. C. F. Wang, R. G. Cassens, W. G. Hoekstra, *J. Food Sci.*, in press.
  12. The air in the animal facilities contained 30 parts per billion  $\text{NO}_2$ , determined according to the method of B. E. Saltzman [in *Methods of Air Sampling and Analysis*, M. Karz, Ed. (American Public Health Association, Washington, D.C., ed. 2, 1977), p. 527]. If all of the inspired  $\text{NO}_2$  were absorbed, metabolized, and excreted as  $\text{NO}_3^-$ , this concentration could account for 1 percent of the excess  $\text{NO}_3^-$  excreted per rat per day.
  13. Urine samples were treated with urease (Sigma

to generate ammonia ( $\text{NH}_3$ ), which is trapped as  $(\text{NH}_4)_2\text{SO}_4$  [E. J. Conway and A. Byrne, *Biochem. J.* **27**, 419 (1933)] and determined on the basis of its reaction with hypochlorite and phenol to form the blue indophenol [H. N. Munro, Ed., *Mammalian Protein Metabolism* (Academic Press, New York, 1969), vol. 3, chap. 30]. The relative abundances of the  $^{15}\text{NH}_4^+$  and  $^{14}\text{NH}_4^+$  were determined by mass spectrometry after oxidation to molecular nitrogen with  $\text{NaOBr}$  (Nuclide 3-60 RMS, State College, Pa.).

14. J. P. Witter and E. Balish, *Appl. Environ. Microbiol.* **38**, 861 (1979).
15. We thank M. McLafferty and W. Rand. This work was supported by National Cancer Institute grants 1 P01 CA26731-01, 2 R26 CA25025-03, RO1 CA15260, and Toxicology Training Grant 2 T32 ES 07020 (to L.G.).

30 September 1980; revised 8 December 1980

## Nitrogen-13-Labeled Nitrite and Nitrate: Distribution and Metabolism After Intratracheal Administration

**Abstract.** Radioactive nitrogen-13 from nitrite ( $\text{NO}_2^-$ ) or nitrate ( $\text{NO}_3^-$ ) administered intratracheally or intravenously without added carrier to mice or rabbits was distributed evenly throughout most organs and tissues regardless of the entry route or the anion administered. Nitrogen-13 from both anions was distributed uniformly between plasma and blood cells. We found rapid *in vivo* oxidation of  $\text{NO}_2^-$  to  $\text{NO}_3^-$  at concentrations of 2 to 3 nanomoles per liter in blood. Over 50 percent oxidation within 10 minutes accounted for the similar nitrogen-13 distributions from both parent ions. The oxidation rates were animal species-dependent. No reduction of  $^{13}\text{NO}_3^-$  to  $^{13}\text{NO}_2^-$  was observed. A mechanistic hypothesis invoking oxidation of  $^{13}\text{NO}_2^-$  by a catalase-hydrogen peroxide complex accounts for the results. These results imply a concentration dependence for the *in vivo* fate of  $\text{NO}_2^-$  or nitrogen dioxide.

The *in vivo* fate of nitrite ( $\text{NO}_2^-$ ) and nitrate ( $\text{NO}_3^-$ ) is being studied with radioactive  $^{13}\text{N}$  (half-life = 10 minutes) tracer technology that offers insight into an enigma of marked contemporary importance. More than 100 years ago, Gamgee (1) first observed what is now known to be the conversion of oxyhemoglobin ( $\text{HbO}_2$ ) to methemoglobin (MetHb) when  $\text{NO}_2^-$  was added to blood. The biochemical pathways of this pharmacologically and toxicologically important transformation are not fully understood (2). Newberne's (3) recent report that long-term  $\text{NO}_2^-$  ingestion by rats caused an increased incidence of cancer in the lymphoreticular system elicited immediate congressional attention (4) because removal of  $\text{NO}_2^-$  as a food additive in accordance with the Delaney Clause may increase the risk of food poisoning from botulism. The resolution (5) of this public health dilemma is complicated by earlier findings (6) that ingested  $\text{NO}_3^-$ , a natural component of many foods, especially vegetables, is reduced to  $\text{NO}_2^-$  by oral microflora to produce salivary  $\text{NO}_2^-$  concentrations of several hundred milligrams per liter. The formation and reactions of  $\text{NO}_3^-$  and  $\text{NO}_2^-$  in the intestinal tract are considered potentially important in understand-

ing the etiology of human gastric cancer, but their significance is controversial (7).

The long-term health effects of  $\text{NO}_3^-$  and  $\text{NO}_2^-$  entering the body through the respiratory tract are largely unknown. These anions may form in the atmosphere (8) or *in vivo* from airborne nitrogenous compounds. Inhalation of nitrogen dioxide ( $\text{NO}_2$ ), the most abundant nitrogenous air pollutant, can result in the formation of  $\text{NO}_2^-$  and  $\text{NO}_3^-$  (9). In a pioneering tracer experiment, Goldstein *et al.* (10) found that  $^{13}\text{N}$  inhaled by rhesus monkeys as  $\text{NO}_2$  gas [0.6 part per million (ppm)] was rapidly taken up by the blood and that a substantial portion was uniformly disseminated to extrapulmonary sites. They postulated from chemical arguments that a portion of the  $\text{NO}_2$  reacted with aqueous vapor and mucus by disproportionation to form nitrous acid ( $\text{HNO}_2$ ) and nitric acid ( $\text{HNO}_3$ ), precursors to  $\text{NO}_2^-$  and  $\text{NO}_3^-$ . Pryor *et al.* (11) found *in vitro* evidence that  $\text{NO}_2$  concentrations below 50 ppm probably react with lung components to form only  $\text{NO}_2^-$ . Svorcova and Kaut (9) observed both  $\text{NO}_3^-$  and  $\text{NO}_2^-$  in the blood of rabbits that had been exposed to 22.5 ppm of  $\text{NO}_2$  for 4 hours. Recently, Igbal and his co-workers (12) observed the *in vivo* formation of a nitrosamine

product in mice that were gavaged with a precursor amine, morpholine, and exposed to  $\text{NO}_2$ . They postulated an  $\text{HNO}_2$  intermediate, although the mechanism was not determined.

In view of the uncertainty about the *in vivo* fate of even simple nitrogenous compounds, it became clear to us that, to reach our ultimate scientific goal of obtaining information about the long-term health effects of  $\text{NO}_2^-$ ,  $\text{NO}_3^-$ ,  $\text{HNO}_2$ , and  $\text{NO}_2$  inhalation, a better understanding of  $\text{NO}_3^-$  and  $\text{NO}_2^-$  pharmacokinetics was needed. Uncertainties about the mammalian economy of nitrogen compounds can be attributed in part to the difficulty of trace  $\text{NO}_2^-$  and  $\text{NO}_3^-$  analyses in biological samples and to the lack of sensitivity intrinsic to stable  $^{15}\text{N}$  tracer and mass-spectrometric detection. The detection limits require quantities of  $^{14}\text{N}$  or  $^{15}\text{N}$  compounds that may perturb normal biochemical processes. We overcame these difficulties by using high-specific-activity ( $1 \times 10^3$  to  $7 \times 10^3$  Ci/mmmole)  $^{13}\text{NO}_2^-$  and  $^{13}\text{NO}_3^-$  for metabolism studies that minimized any pharmacological action of the tracer. Dosages ranged between 10 and 100 ng per kilogram of weight.

The cyclotron target described by Parks and Krohn (13) was used to produce  $^{13}\text{N}$ -labeled  $\text{NO}_3^-$  directly by bombardment of water with protons. Labeled  $\text{NO}_2^-$  was prepared by reduction of  $\text{NO}_3^-$  with an improved copperized cadmium reduction technique described by McElfresh *et al.* (14). All the experiments were done under "no carrier added" (NCA) conditions; however, ubiquitous contamination reduced the specific activity in comparison to that of carrier-free material (15). All solutions for animal experiments were neutralized and made isotonic with phosphate-buffered saline (PBS). Chemical separations (Fig. 1) were accomplished with a high-performance liquid chromatograph (HPLC) fitted with radiation detectors (16).

The experimental animals were Balb/C mice and New Zealand White rabbits, which were fed unlimited amounts of commercial laboratory animal feed and water. Intratracheal (IT) instillation of 15  $\mu\text{l}$  of tracer into mice was done by the Sedgwick and Jahn technique (17). Intravenous (IV) injections were made into a tail vein of the mice or an ear vein of the rabbits.

Our first measurements consisted of organ distribution studies of  $^{13}\text{NO}_3^-$  and  $^{13}\text{NO}_2^-$  in mice; we used 10 to 12 mice for each combination of anion and route of administration. Measurements were made at time intervals of from 5 to 30

minutes between injection and the killing of the animal. Organs were excised within 10 minutes after the death of the animal and weighed. The tracer concentrations in the lungs, heart, kidneys, liver, stomach, small intestine, large intestine, bladder, and carcass were determined by gamma-ray counting.

The time-dependent flux of both tracers achieved transient equilibrium very rapidly for each route of administration but was slightly slower for the lung. The distribution data were relatively constant within 5 minutes after injection (18). The distribution kinetics are time-dependent, because initially all the tracer was isolated at the site of administration and none was in the other organs. However, the principal factor controlling the initial distribution of  $^{13}\text{N}$  from  $\text{NO}_3^-$  or  $\text{NO}_2^-$  is blood flow.

Except for the lungs and carcass, the percentages of  $^{13}\text{N}$ -labeled anion administered per gram (percent A/g) were in-

significantly different at the 5 percent level for each organ, irrespective of whether IT or IV administration was used or the specific anion chosen. Hence, we combined the 4 percent A/g data sets for most organs (mean  $\pm$  the standard error of the mean) to give the following: heart,  $9.1 \pm 1.6$ ; kidneys,  $8.7 \pm 1.1$ ; liver,  $7.5 \pm 0.8$ ; stomach,  $10.0 \pm 3.0$ ; small intestine,  $5.3 \pm 0.5$ ; large intestine,  $7.3 \pm 1.2$ ; and bladder,  $10.5 \pm 5.3$ . The remaining activity varied by route, and the mean  $\text{NO}_2^-$  and  $\text{NO}_3^-$  percent A/g values were distributed as follows: for IV lung,  $8.8 \pm 2.1$ ; IV carcass,  $4.2 \pm 0.3$ ; IT lung,  $26.3 \pm 7.3$ ; and IT carcass,  $3.5 \pm 0.3$ . The higher lung values for the IT administration over our time period were due to the fact that this organ was the site of IT instillation; low activity values for the carcass were due to minimal uptake by the skeleton.

From these  $^{13}\text{N}$  distribution data in the mouse, two possibilities emerged. Either  $\text{NO}_3^-$  and  $\text{NO}_2^-$  distribute equally into the same body space, or  $\text{NO}_3^-$  and  $\text{NO}_2^-$  chemically transform into each other or into sufficiently similar products that no detectable difference in  $^{13}\text{N}$  organ distribution is produced. The even distribution of  $^{13}\text{N}$  also indicates that the  $\text{NO}_2^-$  or  $\text{NO}_3^-$  tracer rapidly reaches a steady-state concentration of no more than 2 to 3 nM in body fluids.

We then examined the distribution of  $^{13}\text{N}$  in blood fractions. Blood samples (0.5 to 1.0 ml) were taken by cardiac puncture from anesthetized mice 10 minutes after IT instillation of  $^{13}\text{NO}_3^-$  or  $^{13}\text{NO}_2^-$ . The samples were separated into cells and plasma by centrifugation. The plasma was further fractionated by precipitation of the plasma proteins (PP) with 50 percent methanol, and the cells were lysed with distilled water and re-centrifuged to remove cellular debris (CD). The lysate was treated with 50 percent methanol and centrifuged to remove the intracellular protein precipitates (CP). There were slight differences in the blood fraction distributions of  $^{13}\text{N}$  from  $^{13}\text{NO}_3^-$  and  $^{13}\text{NO}_2^-$  (Table 1). Three washes of PP, CD, and CP precipitates with PBS solubilized  $\sim 95$  percent of the  $^{13}\text{N}$  and indicated minimal irreversible reaction to form high-molecular-weight products.

We selected the rabbit as a second animal species because earlier experiments with rabbits (9) showed increased blood concentrations of  $\text{NO}_3^-$  and  $\text{NO}_2^-$  after exposure to  $\text{NO}_2$  and because organ distributions in rabbits could be conveniently obtained with our Auger scintillation camera. With intravenous  $^{13}\text{NO}_2^-$

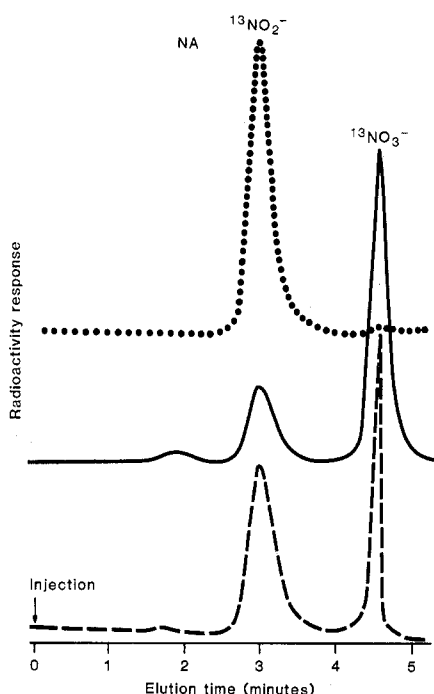


Fig. 1. Radiochromatograms illustrating the oxidation of  $^{13}\text{NO}_2^-$  in mice and rabbits. Anions labeled with  $^{13}\text{N}$  were separated on an HPLC fitted with a Partisil-10 SAX (Whatman) strong anion-exchange column (4.6 mm interior diameter by 250 mm long). The eluent was 30 mM phosphate buffer, pH 3.1; the flow rate was 3.0 ml/min. The 511-keV positron annihilation photons from  $^{13}\text{N}$  were detected with NaI(Tl) crystals. The elution order on this column is nonanionic (NA) labeled compounds,  $^{13}\text{NO}_2^-$ , and  $^{13}\text{NO}_3^-$ . The decay-corrected percentages, given as NA,  $^{13}\text{NO}_2^-$ , and  $^{13}\text{NO}_3^-$ , respectively, for introduced  $^{13}\text{NO}_2^-$  material (dotted line) are 0.2, 99.3, and 0.5; for 10-minute mouse plasma (solid line), they are 3, 27, and 70 (intratracheal instillation); for 10-minute rabbit plasma (dashed line), they are 3, 46, and 51 (intravenous injection).

Table 1. Fractional distribution of  $^{13}\text{N}$  in blood 10 minutes after the administration of  $^{13}\text{NO}_2^-$  or  $^{13}\text{NO}_3^-$ . Standard deviations are given in parentheses.

Blood fractions	Mice*		Rabbits†	
	$\text{NO}_3^-$	$\text{NO}_2^-$	$\text{NO}_3^-$	$\text{NO}_2^-$
Plasma	0.58 (0.05)	0.49 (0.04)	0.62 (0.10)	0.64 (0.08)
Methanol precipitate, plasma proteins	0.12 (0.03)	0.11 (0.03)	0.18 (0.12)	0.10 (0.04)
Supernatant	0.46 (0.03)	0.38 (0.03)	0.44 (0.15)	0.54 (0.06)
Cells	0.42 (0.05)	0.51 (0.04)	0.38 (0.10)	0.36 (0.08)
Water lysate	0.26 (0.06)	0.23 (0.05)	0.21 (0.09)	0.23 (0.05)
Methanol precipitate, intracellular protein	0.07 (0.03)	0.05 (0.03)	0.06 (0.03)	0.05 (0.02)
Supernatant	0.19 (0.04)	0.18 (0.04)	0.15 (0.03)	0.18 (0.07)
Cell debris	0.16 (0.05)	0.28 (0.05)	0.17 (0.07)	0.13 (0.03)

\*Five mice were used for each anion; intratracheal instillation. †Five rabbits were used for the  $\text{NO}_3^-$  and four rabbits for the  $\text{NO}_2^-$  data; intravenous injection.

and  $^{13}\text{NO}_3^-$ , a rapid homogeneous distribution of the radioactivity throughout the rabbit was observed as had been seen in mice. Equilibrium between the intravascular and extravascular compartments was reached within 5 minutes after injection of either radiochemical. The activity was distributed evenly throughout the soft-tissue organs. Only 2 to 3 percent of the  $^{13}\text{N}$  appeared in the urinary bladder during the first 30 to 45 minutes after injection. The blood fraction data for the rabbits (Table 1) are very similar for both anions and are similar to the mouse data.

The hematocrit was about 0.55 for mice and about 0.40 for rabbits. These values were approximately the fractions of tracer found in the cells, suggesting that the  $^{13}\text{N}$  from  $\text{NO}_3^-$  or  $\text{NO}_2^-$  was distributed uniformly on a per-volume basis throughout the blood. Clearly, the  $^{13}\text{N}$ -labeled species are not distributed with the physiological control characteristic of anions such as chloride, which has an extracellular : intracellular ratio of 25 : 1 (19).

Portions of each supernatant from the blood distribution experiments were also analyzed by HPLC (Fig. 1). The chromatographic results obtained from mouse plasma taken 10 minutes after IT instillation of  $^{13}\text{NO}_2^-$  revealed that  $70 \pm 5$  percent (standard deviation) of the  $^{13}\text{N}$  was converted to  $^{13}\text{NO}_3^-$  and  $27 \pm 2$  percent remained as  $^{13}\text{NO}_2^-$ . Nonanionic compounds totaled about  $3 \pm 1$  percent of the activity. One site of  $\text{NO}_2^-$  conversion to  $\text{NO}_3^-$  is the erythrocyte as demonstrated by chromatography of the cell lysate, which showed 100 percent  $^{13}\text{NO}_3^-$ , and chromatography of a PBS cell wash, which showed  $\sim 80$  percent of the activity as  $^{13}\text{NO}_3^-$  and 20 percent as  $^{13}\text{NO}_2^-$ . By comparison, the product distribution in rabbit plasma 10 minutes after  $^{13}\text{NO}_2^-$  IV injection was  $46 \pm 3$  percent  $^{13}\text{NO}_2^-$ ,  $51 \pm 3$  percent

$^{13}\text{NO}_3^-$ , and  $3 \pm 1$  percent nonanionic; these values indicate a slower conversion rate in rabbits than in mice.

Ten minutes after IT instillation of  $^{13}\text{NO}_3^-$  into mice, 100 percent of the  $^{13}\text{N}$  label was found as  $^{13}\text{NO}_3^-$  in all blood fractions. The  $^{13}\text{NO}_3^-$  IV injection data in rabbits exhibited no differences from the mouse IT data. Thus, any  $^{13}\text{NO}_2^-$  formed by the bacterial reduction of  $^{13}\text{NO}_3^-$  was not detected in the blood of either species.

In summary, the very similar organ distributions of  $^{13}\text{N}$ -labeled tracer  $\text{NO}_2^-$  and  $\text{NO}_3^-$  after IT introduction into mice or IV injections into rabbits can largely be explained in terms of the conversion of  $^{13}\text{NO}_2^-$  to  $^{13}\text{NO}_3^-$  in blood. We directly demonstrated that  $\text{NO}_2^-$  was rapidly oxidized to  $\text{NO}_3^-$  under NCA conditions in mice and rabbits, but  $^{13}\text{NO}_3^-$  was not reduced to  $^{13}\text{NO}_2^-$  within the 10-minute observation period. Measurable species differences were observed in the conversion rates of  $\text{NO}_2^-$  to  $\text{NO}_3^-$ .

We hypothesize that under our in vivo conditions (dosages of 10 to 100 ng of  $\text{NO}_2^-$  per kilogram of body weight;  $\text{NO}_2^-$  :  $\text{HbO}_2$  molar ratio in blood of  $10^{-6}$ ), normal spontaneous oxidation of  $\text{HbO}_2$  (2) in erythrocytes produces superoxide ion ( $\text{O}_2^-$ ) and MetHb as demonstrated in vitro by Misra and Fridovich (20). The  $\text{O}_2^-$  is converted by superoxide dismutase (E.C. 1.15.1.1) to hydrogen peroxide ( $\text{H}_2\text{O}_2$ ). This in turn forms a catalase- $\text{H}_2\text{O}_2$  complex, for which  $\text{NO}_2^-$  may act as a substrate, as has been shown to occur in erythrocytes by Cohen and co-workers (22). Chance's earlier work (23) showed the rapid reaction of  $\text{NO}_2^-$  with the catalase- $\text{H}_2\text{O}_2$  complex under physiological conditions and included a postulated mechanism for the oxidation of  $\text{NO}_2^-$  to  $\text{NO}_3^-$ . This schema accounts for our observations. In vitro studies (23) with  $\text{NO}_2^-$  for  $\text{NO}_2^-$  :  $\text{HbO}_2$  molar ratios 2 to 20 million times higher

than our in vivo ratios indicate that  $\text{NO}_2^-$  can react directly with  $\text{HbO}_2$  (23).

Our work demonstrates the in vivo conversion of  $\text{NO}_2^-$  to  $\text{NO}_3^-$  under NCA conditions, and we have found no reactions of  $\text{NO}_3^-$  under similar conditions. Hence, evidence (2, 12, 23) suggesting the direct reaction of  $\text{NO}_2^-$  with hemoglobin or other compounds may result from concentrations of  $\text{NO}_2^-$  or  $\text{NO}_2$  that lead to a saturation of our proposed mechanism; that is, the catalase- $\text{H}_2\text{O}_2$  reaction occurs at  $\text{NO}_2^-$  concentrations below those reported to generate MetHb directly from hemoglobin. Our observation of species differences in  $\text{NO}_2^-$  reaction rates under NCA conditions, coupled with preliminary evidence that bio-transformation mechanisms for  $\text{NO}_2^-$  are concentration-dependent, suggests that adequate extrapolation of animal  $\text{NO}_2^-$  or  $\text{NO}_2$  toxicology data to humans must include interspecies comparison of non-linear pharmacokinetic phenomena (24).

NORRIS J. PARKS

Laboratory for Energy-Related Health Research, School of Veterinary Medicine, University of California, Davis 95616

KENNETH A. KROHN

Department of Radiology, School of Medicine, University of California, Davis

CHESTER A. MATHIS

JOSEPH H. CHASKO

KENNETH R. GEIGER

MARSHA E. GREGOR

Crocker Nuclear Laboratory, University of California, Davis

NEAL F. PEEK

Department of Physics, University of California, Davis

#### References and Notes

1. A. Gamgee, *Philos. Trans. R. Soc. London* **158**, 589 (1869).
2. W. J. Wallace, R. A. Houtchens, J. M. Holt, W. S. Caughey, in *Biochemical and Clinical Aspects of Hemoglobin Abnormalities*, W. S. Caughey, Ed. (Academic Press, New York, 1978), p. 475.
3. P. M. Newberne, *Science* **204**, 1079 (1979).
4. "Does nitrite cause cancer? Concerns about the validity of FDA-sponsored study delay answer" (Report HRD-80-46 by the Comptroller General of the United States, Government Printing Office, Washington, D.C., 31 January 1980).
5. R. J. Smith, *Science* **209**, 1100 (1980).
6. S. R. Tannenbaum, M. Weisman, D. Fett, *Food Cosmet. Toxicol.* **14**, 549 (1976).
7. S. R. Tannenbaum, D. Fett, V. R. Young, P. D. Land, W. R. Bruce, *Science* **200**, 1487 (1978); J. P. Witter, S. J. Gatley, E. Balish, *ibid.* **204**, 411 (1979); S. R. Tannenbaum, *ibid.* **205**, 1332 (1979); J. P. Witter, S. J. Gatley, E. Balish, *ibid.*, p. 1335.
8. B. R. Appel, E. L. Kothny, E. M. Hoffer, G. M. Hidy, J. J. Wesolowski, *Environ. Sci. Technol.* **12**, 418 (1978); J. N. Pitts, Jr., D. Grosjean, K. Van Cauwenbergh, J. P. Schmid, D. R. Fitz, *ibid.*, p. 946.
9. S. Svorcova and V. Kaut, *Cesk. Hyg.* **16**, 71 (1971).
10. E. Goldstein, N. F. Peek, N. J. Parks, H. H. Hines, E. P. Steffey, B. Tarkington, *Am. Rev. Respir. Dis.* **115**, 403 (1977).
11. W. A. Pryor, D. G. Prier, J. W. Lightsey, D. F.

Church, in *Autoxidation in Food and Biological Systems*, M. G. Mimic and M. Karel, Eds. (Plenum, New York, in press).

12. Z. M. Iqbal, K. Dahl, S. S. Epstein, *Science* **207**, 1475 (1980).
13. N. J. Parks and K. A. Krohn, *Int. J. Appl. Radiat. Isot.* **29**, 754 (1978).
14. M. W. McElfresh, J. C. Meeks, N. J. Parks, *J. Radioanal. Chem.* **53**, 337 (1979).
15. The concentration of  $^{13}\text{N}$  from the target was  $\sim 10$  mCi/ml as  $\text{NO}_3^-$  and variable amounts of  $\text{NO}_2^-$  and ammonium ( $\text{NH}_4^+$ ) radiochemical impurities at the end of bombardment. Only radiochemical preparations with  $> 97$  percent  $^{13}\text{NO}_3^-$  were used for animal experiments. We used a rapid concentration and purification technique with high-performance anion exchange (J. H. Chasko and J. R. Thayer, in preparation) to remove any ammonia ( $\text{NH}_3$ ) formed in the reduction procedure. The technique resulted in solutions with  $^{13}\text{N}$  concentration  $> 150$  mCi/ml and a radiochemical purity of  $> 99$  percent.
16. K. A. Krohn and C. A. Mathis, in *Short-Lived Radionuclides in Chemistry and Biology*, K. A. Krohn and J. W. Root, Eds. (American Chemical Society, Washington, D.C., in press).
17. C. Sedgwick and S. Jahn, *Calif. Vet.* **34**, 27 (1980).
18. The time dependence of the distribution data was analyzed with a simple linear least-squares regression model: percent  $A(t) = mt + b$ , where percent  $A(t)$  is the percentage of administered dose in each organ at time  $t$ , and  $m$  and  $b$  are the calculated slope and intercept, respectively. With one exception (IT lung), the slopes for all the various combinations of organs and tracer ions were not significantly different from zero at the 5 percent level in both the IT and IV experiments. For both anions, the IT lung data gave a coefficient of determination indicating that only  $\sim 18$  percent of the dispersion could be associated with time.
19. A. C. Guyton, *Textbook of Medical Physiology* (Saunders, Philadelphia, ed. 4, 1971), p. 380.
20. H. P. Misra and I. Fridovich, *J. Biol. Chem.* **247**, 6960 (1972).
21. G. Cohen, M. Martinez, P. Hochstein, *Biochemistry* **3**, 901 (1964).
22. B. Chance, *J. Biol. Chem.* **182**, 649 (1950).
23. F. L. Rodkey, *Clin. Chem. (N.Y.)* **22**, 1986 (1976); H. Kosaka, K. Imaizumi, K. Imal, I. Tyuma, *Biochim. Biophys. Acta* **581**, 184 (1979).
24. We are addressing this question with  $^{13}\text{N}$  tracer techniques similar to those described earlier but with logarithmically increasing amounts of added carrier.
25. Research supported by the California Air Resources Board, the National Science Foundation, and the U.S. Department of Energy. We thank G. Vial, M. Al-Bayati, J. C. Meeks, J. R. Thayer, E. Profita, and L. A. Swartz for experimental assistance and H. P. Misra, W. D. Brown, L. S. Rosenblatt, and G. F. Russell for reviewing the manuscript.

24 November 1980

## Inherited Primary Hypothyroidism in Mice

**Abstract.** A new autosomal recessive mutation that causes hypothyroidism has been identified in mice. The gene, herein named hypothyroid (*hyt*), has been mapped on chromosome 12 approximately 30 units from the centromere. The mutants are characterized by retarded growth, infertility, mild anemia, elevated serum cholesterol, very low to undetectable serum thyroxine, and elevated serum thyroid-stimulating hormone. Thyroid glands are in the normal location but are reduced in size and hypoplastic. Mutant mice respond to thyroid hormone therapy by improved growth and fertility. These findings suggest that the *hyt* mutant gene results in primary hypothyroidism unresponsive to thyroid-stimulating hormone.

Congenital hypothyroidism is a recognized cause of retarded somatic and neurological development in mammals. Among human beings, this glandular malfunction occurs once in every 3684 births (1). Approximately two-thirds of affected infants have primary hypothyroidism, indicated by findings of depressed serum thyroxine ( $\text{T}_4$ ), elevated serum thyroid-stimulating hormone (TSH), and hypoplastic or, more rarely, ectopic thyroid glands (2). The resulting cretinism can be prevented only by immediate hormone replacement therapy. Although the explanation for the triad of low serum  $\text{T}_4$ , elevated serum TSH, and hypoplastic thyroids is not conclusively established, three reports provide important clues to one possible mechanism: Stanbury *et al.* (3) reported on an 8-year-old boy with congenital hypothyroidism in the absence of goiter, who was unresponsive to exogenous TSH; Medeiros-Neto *et al.* (4) described a 19-year-old male with identical symptoms and showed that neither thyroidal radioiodine uptake nor function of adenosine 3', 5'-monophosphate increased with exogenously administered TSH; Codaccioni *et*

*al.* (5) discovered similar features in a 17-year-old male and showed that TSH receptors were present, but activation of thyroid adenylate cyclase was deficient. These observations support the idea that thyroid hypoplasia and hypofunction in some patients may result from failure of thyrofollicular cells to respond to endogenous TSH. That such a situation may arise from a genetic event has been suggested in reports of nongoitrogenic hypothyroidism in siblings or in parents and their offspring (6). We now report a new recessive mutation in laboratory mice (named hypothyroid, gene symbol *hyt*) that causes hypothyroidism in the absence of goiter.

The mutant phenotype was first observed in a sib-mated pair of RF/J mice (Animal Resources colonies, the Jackson Laboratory) when the female failed to grow or reproduce. A small research colony was established by mating the normal male parent to normal RF/J females, followed by backcrossing female offspring to the sire and by sibling matings of the original pair. In addition, we began the transfer of the mutant gene by outcrossing to BALB/cByJ mice to cir-

cumvent the poor reproductive performance of RF/J mice and to test the effects of the mutant gene on a heterogeneous background.

The hypothyroid phenotype was due to an autosomal recessive mutation, because the mating of a normal individual to an affected female or male whose fertility had been restored (see below) resulted in all normal young and the intercrossing of these young produced approximately 25 percent affected individuals (1047 normal and 325 mutant). Positive genetic linkage was found with the metacentric Robertsonian chromosomal translocation *Rb(8.12)5Bnr* (hereafter *Rb5Bnr*). First filial generation (*Rb5Bnr*  $+/+$  *hyt*) females were mated to *hyt/hyt* males, and the resultant offspring were classified visually for the *hyt* phenotype and chromosomally for the *Rb5Bnr* translocation (7). Of 141 offspring, 102 were of a parental phenotype (31, *Rb5Bnr*  $+/+$ ; 71,  $+/$  *hyt*) and 39 were of a crossover phenotype (17, *Rb5Bnr* *hyt*; 22,  $+/+$ ). Therefore *hyt* is linked to the *Rb5Bnr* translocation and carried at the proximal end of chromosome 8 or 12 at a distance of  $27.7 \pm 3.8$  map units from a centromere (8). Since *hyt* did not show linkage to the *Os* gene located on chromosome 8 approximately 25 map units from its centromere, we conclude that *hyt* is located on chromosome 12.

Retarded growth was consistently observed in RF/J and BALB/cByJ-N1F2 outcross mutant mice at weaning (3 weeks of age). This deficiency became more pronounced during the rapid growth rate of the pubertal period. Weekly body weight data obtained on 18 BALB/cByJ-N1F2 litters, toe-clipped at birth for later genotype identification, revealed that *hyt/hyt* mice weighed significantly less than their normal littermates by 22 days of age (Fig. 1). A study of *hyt/hyt* mice and their normal littermates was conducted to determine whether a diet supplemented with desiccated thyroid powder could initiate growth and restore fertility, as has been demonstrated with Snell's dwarf (*dw/dw*) mice (9). Weekly body weight data obtained from weanling N1F2-*hyt/hyt* and  $+/+$  littermate mice fed either 0.025 percent desiccated thyroid powder or control diet (Fig. 1) showed that (i) thyroid replacement induced rapid catch-up growth in *hyt/hyt* mice, (ii) *hyt/hyt* mice displayed a very low rate of growth without thyroid therapy, and (iii) normal mice were not affected by the treatment. After 4 to 5 weeks of treatment with desiccated thyroid, *hyt/hyt* mice were phenotypically similar to  $+/+$  controls,